




Cite this: *J. Mater. Chem. B*, 2023, 11, 1545

Acid-assisted polymerization: the novel synthetic route of sensing layers based on PANI films and chelating agents protected by non-biofouling layer for Fe²⁺ or Fe³⁺ potentiometric detection†

Rimeh Ismail, Ivana Šeděnková, Jan Svoboda,  Miroslava Lukešová, Zuzana Walterová and Elena Tomšík  *

A new synthetic method for the fabrication of a sensing layer is presented. PANI films as an ion-to-electron transducer were prepared via acid-assisted polymerization in concentrated formic acid (HCOOH) in the presence of ethanol and ammonium persulfate (APS, as the initiator). The ratio of monomer to ammonium persulfate was 1:0.1. 2,2-Bipyridyl, 1,10-phenanthroline-5-amine, and 8-hydroxyquinoline were used as chelating agents that can complex Fe²⁺ or Fe³⁺ ions. The proposed sensors demonstrated an appropriate reproducibility with a rapid response to the presence of Fe²⁺ or Fe³⁺ ions, even at $T \sim 37^\circ\text{C}$. It was revealed that the method of deposition of a chelating molecule affects the response of sensors. The *in situ* deposition during acid-assisted polymerization leads to a fast response compared to the layer-by-layer deposition. PMeOx/X₁-PANI@FTO and PMeOx/Z₁-PANI@FTO sensors exhibit rapid response and are considered a promising detection layer for Fe²⁺ or Fe³⁺ ions respectively. We envision that this system can contribute to the next generation of advanced bio-sensors for the potentiometric detection of iron.

Received 9th November 2022,
Accepted 8th January 2023

DOI: 10.1039/d2tb02450k

rsc.li/materials-b

Introduction

Since the discovery of conducting polymers, polyaniline has received high attention and has become a particular focus of interest because of its wide application potential (adsorption, catalysis, gas sensors, composite fabrications, *etc.*) and its considerable advantages including ease of synthesis, low cost, good environmental stability and excellent performance.^{1–4} Several methods have been introduced for the fabrication of PANI containing various types of nanostructures (nanospheres, nanogranules, nanorods, nanoflowers, nanofibers, and nanotubes) with different properties.^{5–9} It has been reported that the synthesis of PANI is strongly influenced by aniline polymerization conditions, such as the oxidant, solvent, electrode material, pH of the electrolyte, temperature, chemical additives (oligoaniline and π bonding compounds), electrolyte composition, dopant anions, *etc.*^{10–16} which are of great significance for controlling the polymerization and adjusting the molecular structures and the properties of polyaniline. Therefore, the optimization of the synthesis

condition of PANI with specific physicochemical properties for good performance applications is very important. PANI can be prepared by different approaches such as chemical, electrochemical, electrospinning or templated polymerization.^{17–21} For example, a templated method can be used to obtain multiple nanostructural polyanilines such as zero-dimensional nanospheres, one dimensional nanotubes, nanofibers and nanorods and two-dimensional, nanosheets.^{20,22} However, polyanilines produced by electrodeposition, templated method or electrospinning are limited because of their low yield and fussy postprocessing.²³ Chemical oxidative polymerization has a large potential to be used in the field of synthesis technology and is recognized as the major route for producing PANI with controllable size and morphology. In this route, the evolution of polymerization can be observed. In the beginning the mixture has no color, which turns to blue and dark blue when dimers and oligomers produced.²⁴ Generally, PANI is widely prepared by the conventional oxidative polymerization of aniline with ammonium persulfate (APS) in a concentrated acid solution (HCl) or a weaker acid (acetic acid). Thus, several approaches for preparation of PANI films have been reported.^{24–29} But the polymerization process of the desired morphologies and structures still represents a significant challenge.

The current work is motivated by the fact that PANI has gained a lot of interest in the fabrication of various sensors and

Institute of Macromolecular Chemistry AS CR, Heyrovského nám. 2, 162 06 Prague 6, Czech Republic. E-mail: tomsik@imc.cas.cz

† Electronic supplementary information (ESI) available: Evolution of molecular weight of PANI measured by MALDI-ToF. See DOI: <https://doi.org/10.1039/d2tb02450k>



biosensors owing to the richness of synthesis of PANI, and considering that until now, no study related to the preparation of PANI films by acid-assisted polymerization in the presence of ethanol, has been reported so far. It describes a new synthetic way of sensing layer preparation based on PANI films and chelating molecules, coated by a non-biofouling layer made of poly(2-methyl-2-oxazoline) (PMeOx) for the monitoring of Fe(II) and Fe(III) ions. Firstly, a stable PANI solution was successfully prepared by acid-assisted polymerization, while, three chelating molecules (2,2-bipyridyl, 1,10-phenanthroline-5-amine, and 8-hydroxyquinoline) were deposited on top of the PANI layer using two methods (drop-casting deposition and *in situ* deposition during polymerization). These two methods were investigated by cyclic voltammetry (CV) and electrochemical impedance spectroscopy (EIS) in order to evaluate the electrochemical performance of the developed sensing films. The next step was to coat/protect the developed sensing layer with the non-biofouling layer consisting of poly(2-methyl-2-oxazoline). The final sensing layers were investigated using a potentiometric technique for its ability to detect Fe²⁺ or Fe³⁺ ions respectively at room temperature or/and 37 °C.

Results and discussion

Synthesis, assembly, and characterization of the sensing layers

In the current work we discovered a new chemical method of aniline synthesis, which leads to the formation of stable PANI suspension that could be deposited on any desirable surface. The Video SV1 (ESI†), shows the PANI suspension after 6 months. A brief description of the acid-assisted polymerization is as follows: aniline monomer is dissolved in concentrated formic acid and a really small amount of the APS dissolved in water is added (ratio aniline:APS is 1:0.1). In the discovered synthetic procedure, the APS is not an oxidant (as is usually presented for semiconducting polymer) but rather an initiator. After 10 min, the reaction turns to a dark-green color, as is usually observed in the synthesis of PANI when the monomer to oxidant ratio is 1:1. In our case, the ratio of aniline:APS is 1:0.1, ten times less. To study the mechanism of aniline polymerization (formation of cation radicals), the EPR signal was recorded for 24 h, and the results are presented in Fig. 1. It is well known that the formation of cation radicals in PANI is either during chemical synthesis or when it's in the oxidized/protonated form.³⁰ The presence of cation radicals in the polymer structure is connected with the mechanism of electron charge transfer. The electron paramagnetic resonance (EPR) signal (Fig. 1) of aniline solution measured at $t = 0$ h and 24 h shows the presence of a sharp and narrow peak located at the 3355 G, confirming the presence of cation radicals in the solution already from the beginning of aniline polymerization. Based on these results we conclude that aniline polymerization proceeds (initiation and propagation) *via* the formation of cation radicals. However, to obtain the PANI it is not necessary to have a high concentration of APS, as has been reported in the literature so far. Note that the intensity of the peak increased

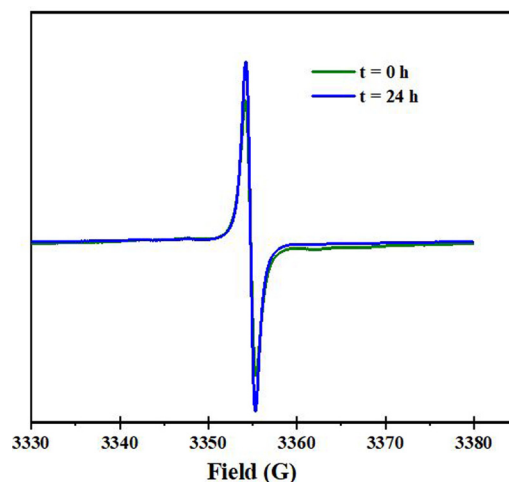


Fig. 1 EPR spectra of PANI solution at $t = 0$ h and $t = 24$ h.

after 24 h whereas the peak width Δ remained constant (see Fig. 1).

It worth emphasizing that aniline polymerization in concentrated formic acid leads to the formation of a stable PANI suspension – no precipitate is formed even after 6 months (see Video ESI† SV 1a–c). The PANI film could be obtained from this PANI suspension at any desired surface simply by evaporation of the formic acid at room temperature. Moreover, the new acid-assisted polymerization method could be used to obtain composite film if at the beginning of the polymerization the desired additive is inserted. That was tested in the current work also.

The next step was to determine the molecular weight of PANI chains during acid-assisted polymerization. The matrix-assisted laser desorption/ionization time-of-flight mass spectrometry (MALDI-TOF) data (negative ionization mode was applied) are recorded for solutions immediately after mixing aniline and APS and after 48 h (see Fig. 2a). The detailed investigation of aniline solution is presented in the ESI† Fig. S1.

It is observed that already at the beginning of polymerization ($t = 0$ h) oligomers are formed with $m/z = 542, 633$ and 977 , corresponding to hexamer, heptamer, and decamer. After 48 h (Fig. 2a), oligomers with longer chains were observed which can be assigned to the PANI with 11, 12, and 13 repeat units ($m/z = 970, 1059$, and 1149 , respectively). Between 24 h and 48 h, the molecular weight did not increase, meaning that the reaction is complete after 24 h (see the ESI† Fig. S1). From these results we can underline that the molecular weight of PANI chains prepared by acid-assisted polymerization mainly consists of oligomers. These oligomer chains are well-dissolved in concentrated formic acid, and that is why PANI suspension is stable even after 6 months: no precipitation is observed.

The chemical structure of the PANI film prepared by acid-assisted polymerization was confirmed by X-ray photoelectron spectroscopy (XPS) analysis (see Fig. 2b). The XPS element full scan spectrum is presented in the ESI† Fig. S2. The XPS spectrum of N 1s was deconvoluted into the following component peaks: the signal located at ~ 399.1 eV, is assigned to



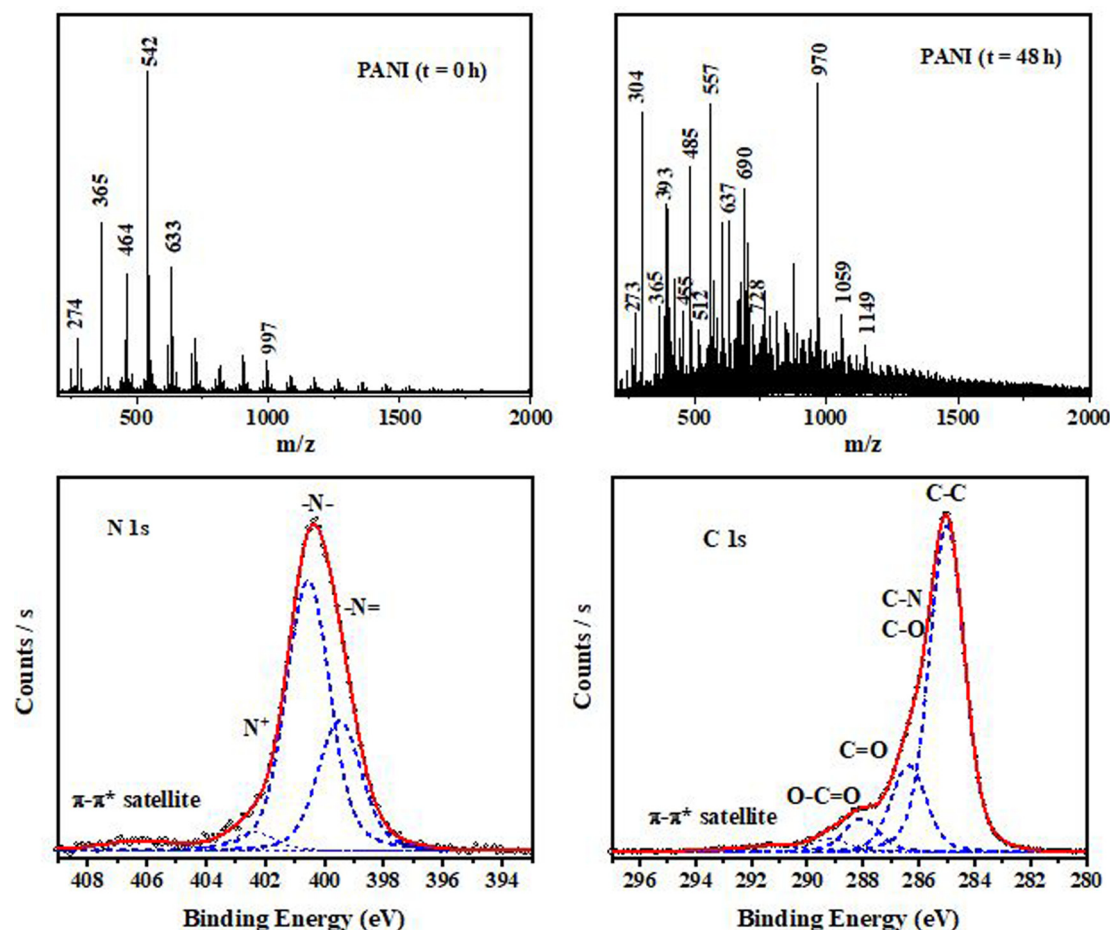


Fig. 2 (a) MALDI-TOF measurements recorded at $t = 1$ h and 48 h of PANI solution prepared by acid-assisted polymerization, and (b) the N 1s and C 1s deconvoluted XPS spectra of PANI@FTO.

imine group $-N=$ and the signal at ~ 400.6 eV to the secondary amine group $-NH-$.³⁵ The peak at 402.4 eV corresponds to positively charged nitrogen atoms.^{31–35} The deconvolution of the peak C 1s exhibits four peaks (Fig. 2b). The major peak at 285.0 eV can be associated with (C-C/C-H); the peak observed at 286.4 eV can be attributed to (C-N/C-O), the peak at around 288 eV to C=O, and the peak appearing at 289.3 eV can be assigned to O-C=O.³⁶

Since the PANI film was synthesized *via* the acid-assisted polymerization method, it is interesting to investigate the electrochemical properties of the PANI film. The cyclic voltammetry measurement of the PANI film deposited at the FTO support was recorded and the result is shown in Fig. 3. The electrochemical performance of the PANI film is measured in 0.1 M H_2SO_4 in the range between -0.1 and 0.8 V *versus* the Ag/AgCl reference electrode, and proves that we obtained PANI with the oxidation and reduction peaks similar to the one reported in the literature for PANI obtained using other methods (chemical or electrochemical);^{35–37} it means that the PANI film obtained by our new technique could be used as the ion-to-electron transducer.

In general, we conclude that we have discovered a new method to polymerize aniline by acid-assisted polymerization

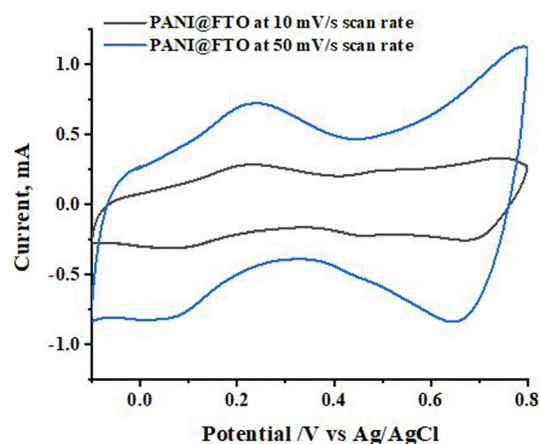
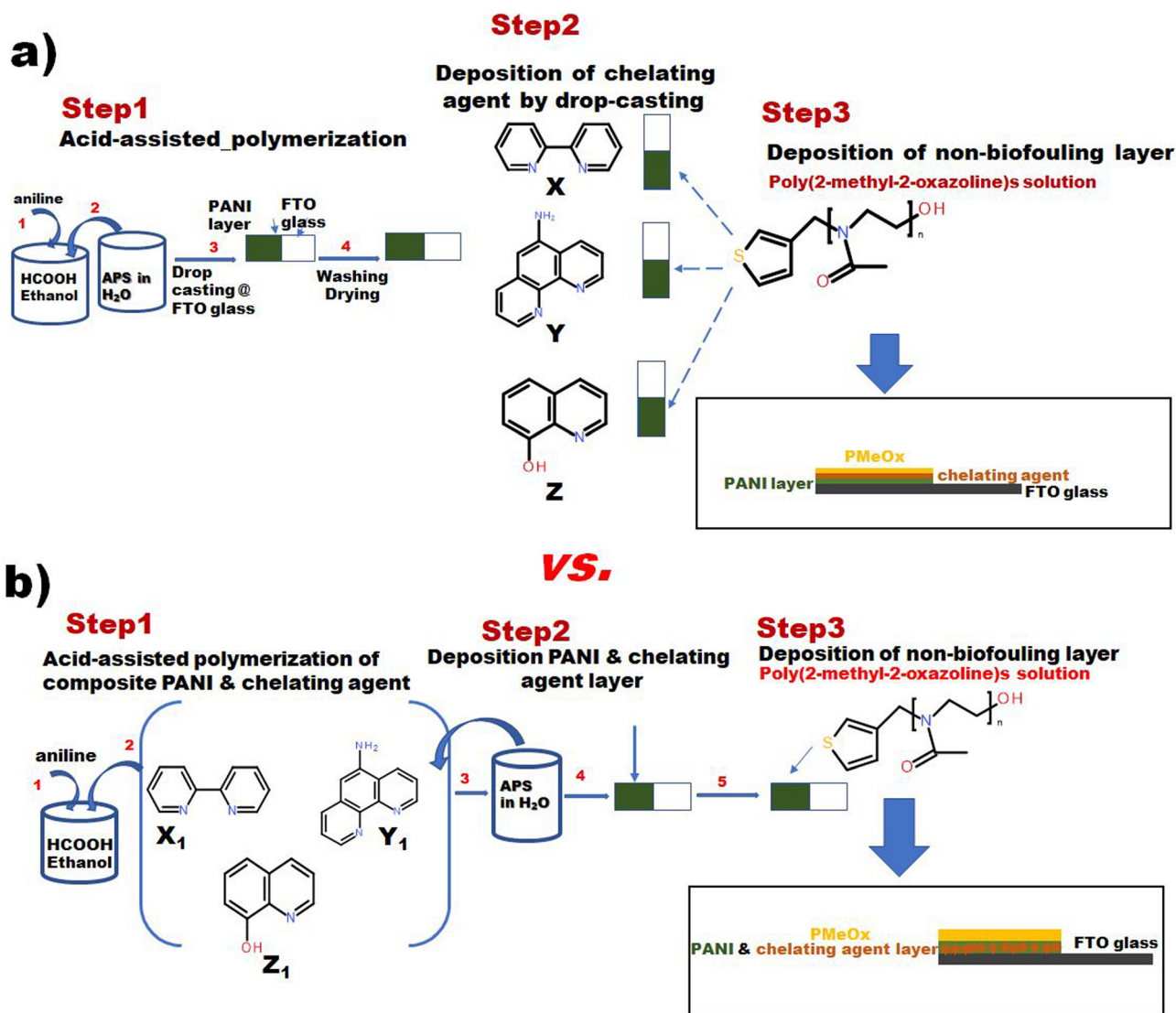


Fig. 3 Cyclic voltammetry curves of PANI@FTO recorded at different scan rates 10 and 50 $mV s^{-1}$, in 0.1 M H_2SO_4 .

with the formation of a stable PANI suspension, which could be deposited as a thin layer on any support (conducting or non-conducting). Such polymerization technique has not been reported in the literature so far.





Scheme 1 (a) The procedure of the sensing layer assembly: acid-assisted polymerization of PANI solution and deposition on FTO, then drop-casting deposition of the chelating molecule, and deposition of non-biofouling poly (2-methyl-2-oxazoline) layer, and (b) the procedure of sensing layer preparation: *in situ* integration of chelating molecules during acid-assisted polymerization of aniline and deposition of the non-biofouling poly(2-methyl-2-oxazoline) layer.

The next goal was a deposition of the chelating molecules in order to chelate/detect either Fe^{2+} or Fe^{3+} ions. Three chelating molecules were applied: 2,2-bipyridyl, 1,10-phenanthroline-5-amine and 8-hydroxyquinoline. The deposition was accomplished by two methods: (1) deposition of the individual chelating solution on top of PANI film and its fixation by cyclic voltammetry (see Scheme 1a), and (2) *in situ* incorporation of chelating molecules to the structure of PANI suspension with the following deposition of the composite film (see Scheme 1b). The details of the applied solvents and experimental conditions are presented in the Experimental part and Table 2, and as a roadmap in the ESI† Fig. S3. Importance of the discovery of acid-assisted polymerization method for PANI suspension synthesis lay in the fact that a really small amount of the initiator is used. The PANI film is formed easily at any surface simply by evaporation of the formic acid at room

temperature. After PANI film deposition is complete it is washed to remove the residual of the initiator and/or formed by-products.

The electrochemical and potentiometric performances of the developed sensors obtained by these two methods are investigated and the results are shown below.

Firstly, to prove that chelating molecules were successfully attached to the PANI film Raman spectroscopy measurements were conducted for PANI and the corresponding composites: X-PANI@FTO, Y-PANI@FTO, Z-PANI@FTO, X₁-PANI@FTO, Y₁-PANI@FTO, Z₁-PANI@FTO, and the results are presented in Fig. 4. All spectra, independent of the method of application of chelating agents, confirm the formation of PANI films. The main bands at about 1600 cm^{-1} and 1500 cm^{-1} are connected with the C=C bending vibration in quinoid rings and the C=N stretching vibration of imine sites, respectively.



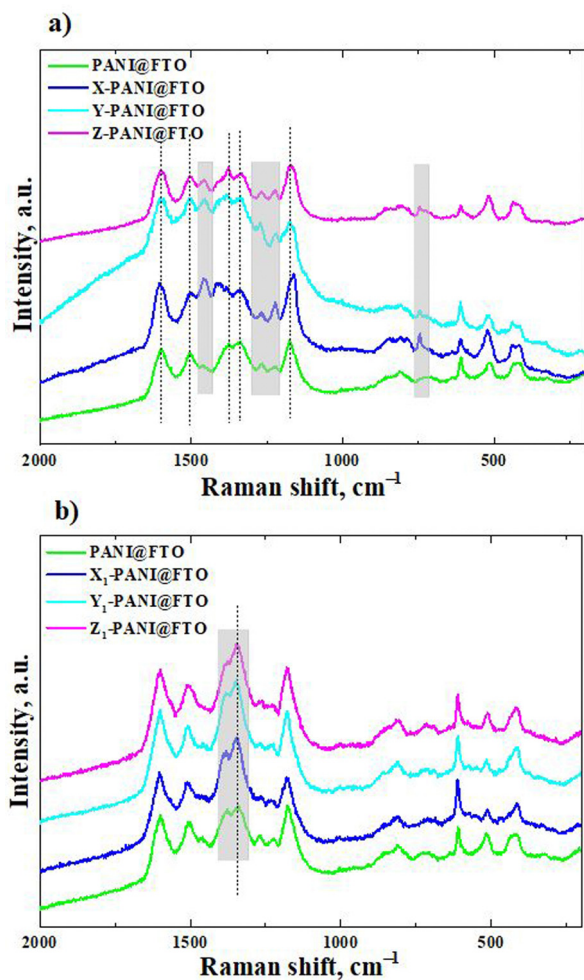


Fig. 4 Raman spectroscopy (excitation laser of 785 nm) (a) PANI@FTO, X-PANI@FTO, Y-PANI@FTO and Z-PANI@FTO; and (b) PANI@FTO, X₁-PANI@FTO, Y₁-PANI@FTO, and Z₁-PANI@FTO.

The strong band at around 1176 cm^{-1} is assigned to the C–N stretching in protonated emeraldine structures.

The changes in the molecular structure of the PANI film after the drop-casting of the chelating molecules are reflected in their Raman spectra (Fig. 4a). The spectral features are connected with the presence of uncharged imine sites. The new band at $\sim 1455\text{ cm}^{-1}$ is observed linked to the stretching vibration of the imine grouped in the emeraldine base.

The band at 744 cm^{-1} is then connected with the imine deformation of the C–N–C structure. Raman spectroscopy is the general surface-sensitive method. The changes in the spectra of the samples prepared by the layer-by-layer deposition reflect the surface of the PANI film in interaction with the chelating agents.

The incorporation of the chelating molecules in the PANI suspension does not have any significant effect on the Raman spectra of the PANI films (Fig. 4b). The spectra are close to the spectrum of PANI prepared in the concentrated formic acid.

The only increase in the intensity of the band observed at 1350 cm^{-1} that can be attributed to the symmetric stretching

vibration of protonated C–N⁺ segments with the bond intermediate between single and double prevalent in the leucoemeraldine form of PANI.³⁸

Furthermore, characterization of the composite film based on PANI and chelating molecules, and the effect of the non-biofouling layer on the electrochemical performance, cyclic voltammetry (CV) measurement with a scan rate of 50 mV s^{-1} and electrochemical impedance spectroscopy (EIS) at the open circuit potential, was carried out. The results of the measurements are presented in Fig. 5 and 6.

The CV of the PANI@FTO electrode was measured in $0.1\text{ M H}_2\text{SO}_4$ with a scan rate of 50 mV s^{-1} . In the current study, only one scan rate is chosen in order to analyze the interaction of the chelating molecules with PANI and the effect of the non-biofouling layer (PMeOx) on the electrochemical properties.

The CV of PANI has two redox peaks similar to the one reported in the literature for PANI obtained using other methods.³⁹ The deposition of the chelating molecules by the drop-casting method (see Fig. 5a) changed the profile of the CV curves. In particular, the first oxidation peak is shifted to higher oxidation potentials. Such behavior is explained by the interaction of the PANI film with the chelating molecules. It must be emphasized that all chelating molecules affect the CV of PANI in a similar way (see Fig. 5a). On the other hand, if chelating molecules were incorporated into PANI during *in situ* acid-assisted polymerization, the change in the CV was observed only for X₁-PANI@FTO and Z₁-PANI@FTO developed electrodes (see Fig. 5c). Y₁-PANI@FTO electrode shows similar CV to the one obtained for PANI.

This tendency is explained by the chemical nature of the chelating molecule (1,10-phenanthroline-5-amine). The chelating 1,10-phenanthroline-5-amine has an amino group in its structure similar to aniline (see Table 2).

Based on this knowledge we proposed that 1,10-phenanthroline-5-amine could also participate in the oxidation/reduction process: the amino group could be oxidized and reduced. The deposition of the protected layer – PMeOx – has a small impact on the electrochemical performance of the developed sensing films: the total oxidation and reduction currents decreased due to the blocking of the surface by the PMeOx film, see Fig. 5b and d.

The EIS of the developed sensing films was studied and used as the proof of interaction between chelating molecules and PANI from one hand, and as the successful deposition of a non-biofouling layer on top of the X-PANI@FTO, Y-PANI@FTO, Z-PANI@FTO, and X₁-PANI@FTO, Y₁-PANI@FTO, Z₁-PANI@FTO electrodes. The results of the recorded data are presented in Fig. 6.

The EIS is a powerful method of analyzing the complex electrical resistance of a system and is sensitive to surface phenomena and changes of bulk properties, as well as for determining capacitance or diffusion of ions at the surface.

Fig. 6 shows the EIS measurements of net PANI film, PANI films with the chelating molecules (two methods of the depositions), and developed sensing electrodes (chelating molecules/PANI@FTO). It is obvious that the Nyquist plots



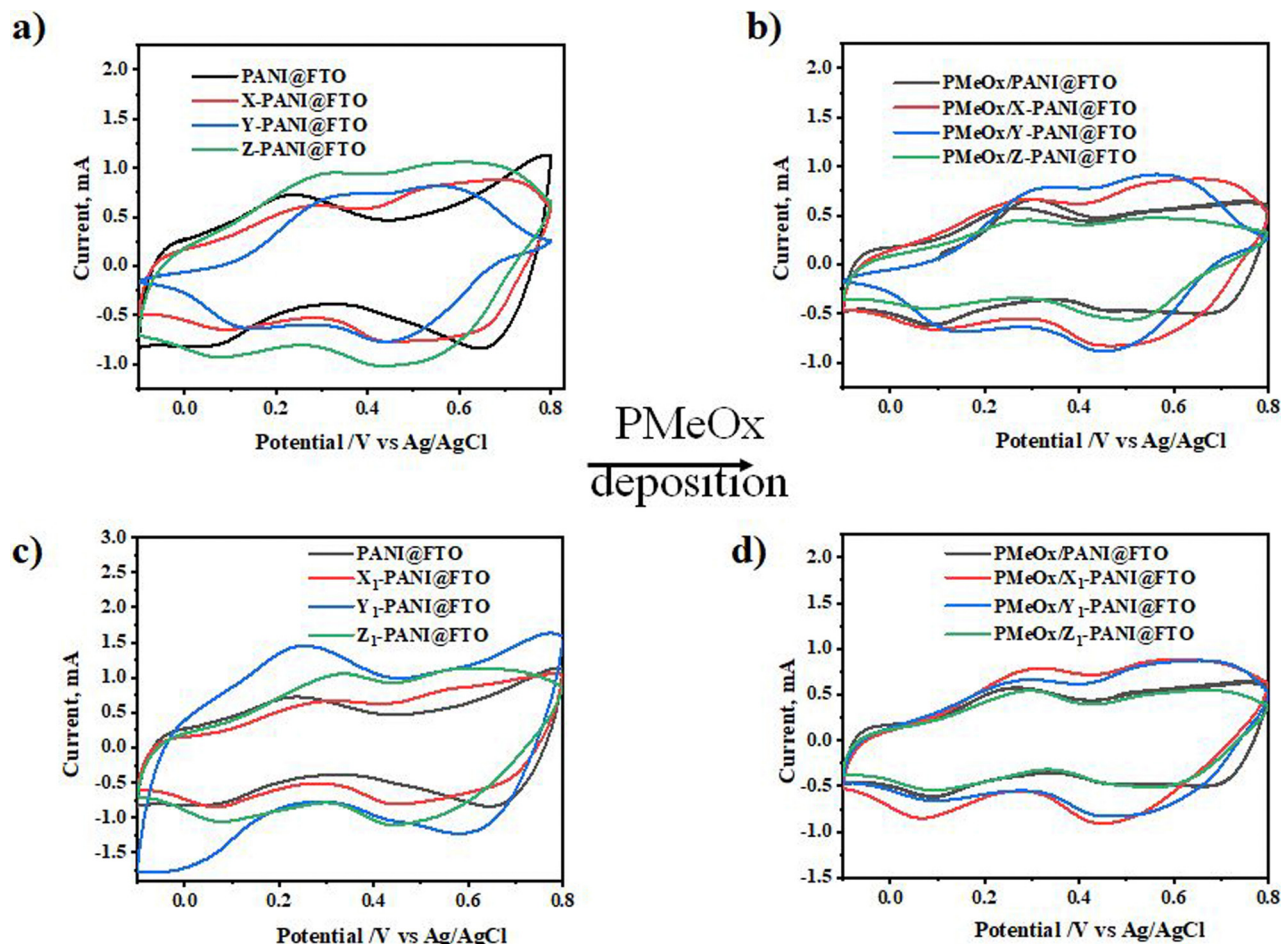


Fig. 5 Cyclic voltammograms of developed electrodes recorded at a 50 mV s^{-1} scan rate in the potential window from -0.1 V to 0.8 V vs. the Ag/AgCl reference electrode in $0.1 \text{ M H}_2\text{SO}_4$.

change after chelating molecule deposition, see Fig. 6a and c. In particular, the high value of the impedance is recorded for the PANI film, and after chelating molecules were deposited the imaginary part of the impedance decreased, proving the successful attachment of the chelating molecules towards PANI. It is also confirmed that the PMeOx layer was deposited on top of X-PANI@FTO, Y-PANI@FTO, Z-PANI@FTO, and X₁-PANI@FTO, Y₁-PANI@FTO, Z₁-PANI@FTO electrodes (see Fig. 6b and d).

The impedance spectra were analyzed using equivalent circuits, which is summarized in the Table 1.

In our case, two equivalent circuits were applied, which consist of resistance, capacitance, Warburg impedance, and constant phase element (CPE) connected either in parallel or in series.

The total resistance of the system (which includes resistances of the electrolyte and film) is 27Ω for PANI@FTO, and slightly decreases after chelating molecule deposition. It must be emphasized that the deposition of the non-biofouling layer only marginally changes the resistance of the developed electrodes. It means that the protected PMeOx layer does not decrease the electrochemical performance of the developed sensing layers. The capacitance of the developed sensing films does not decrease dramatically after the introduction of the

chelating molecules and PMeOx, compared to the literature data.^{40,41} Such behavior is explained by the formation of the thin film of PMeOx on top of PANI film.

The method of chelating molecule deposition plays an important role in the proposed circuit models: when it is drop-casting – the resistance is connected in series with the capacitance; on the other hand, if it is *in situ* acid-assisted deposition – the resistance is connected parallel to the capacitance.

The corresponding sum of squares of the relative residuals (χ^2 value) for the fitting parameters could be found in Table 1. The small value of the χ^2 proves that proposed models could be applied to describe the composite films.

Potentiometric detection of the sensing layers towards Fe^{2+} and Fe^{3+} ions

In our study, new sensing layer for detection of Fe^{2+} or Fe^{3+} ions were produced. The chelating layer (which can detect selectively iron ions) was deposited by two methods (see Table 2 and Schemes 1a and b). In order to investigate the effect of the deposition method of chelating molecules on the response of the sensing layer to the presence of Fe^{2+} or Fe^{3+} ions, a potentiometric analysis was done in a 0.1 M solution of NaCl.



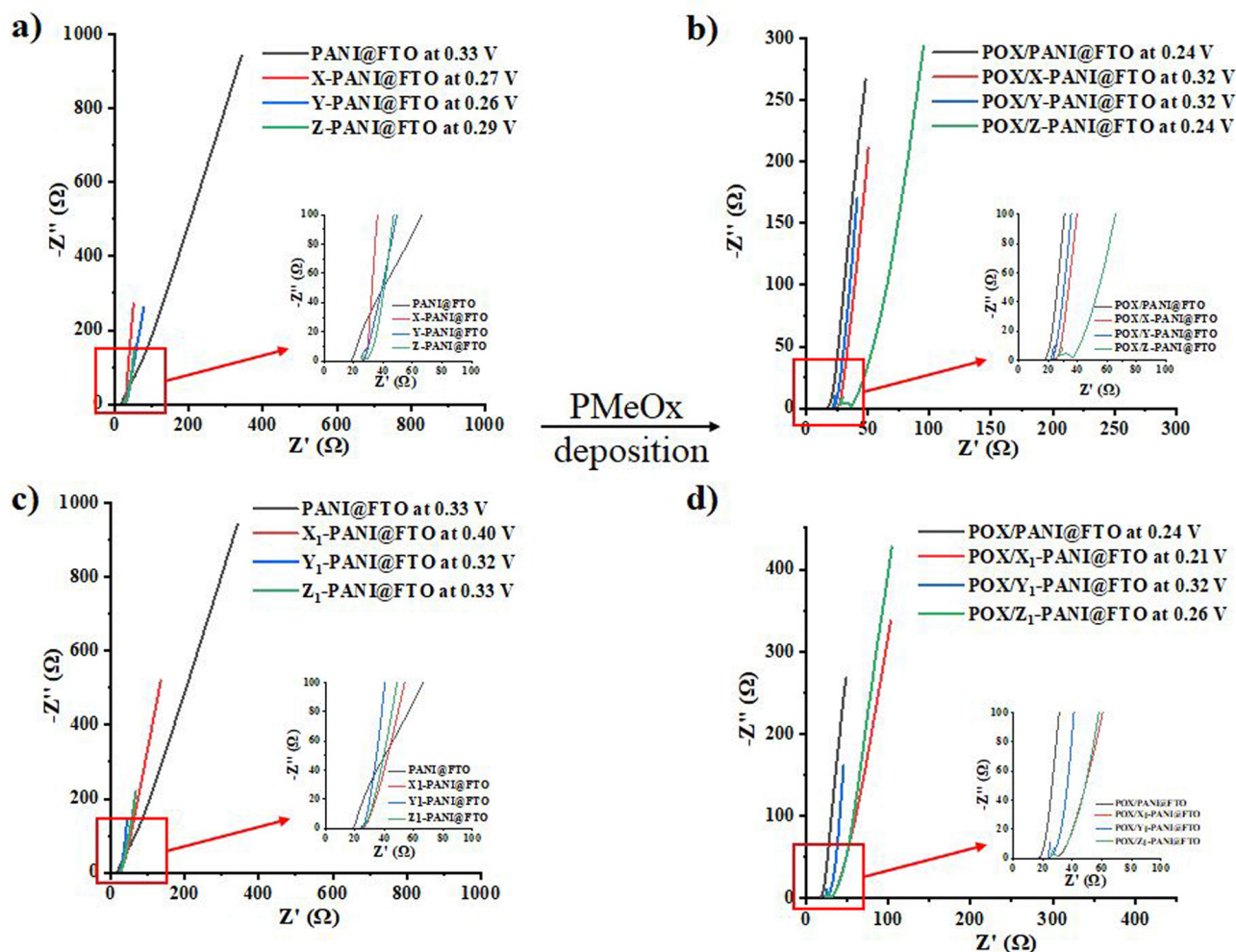


Fig. 6 Nyquist plots of developed (a) PANI@FTO, X-PANI@FTO, Y-PANI@FTO, Z-PANI@FTO, (b) PMeOx/PANI@FTO, PMeOx/X-PANI@FTO, PMeOx/Y-PANI@FTO, PMeOx/Z-PANI@FTO, (c) PANI@FTO, X₁-PANI@FTO, Y₁-PANI@FTO, Z₁-PANI@FTO, and (d) PMeOx/PANI@FTO, PMeOx/X₁-PANI@FTO, PMeOx/Y₁-PANI@FTO, PMeOx/Z₁-PANI@FTO electrodes measured in 0.1 M HCl at open circuit potentials.

The precaution was taken for the potentiometric detection of Fe^{2+} ions; particularly, the studied solution was purged with nitrogen gas to eliminate dissolved oxygen. This procedure is necessary in order to avoid the oxidation of Fe^{2+} ions to Fe^{3+} ions.

Based on our previous work,⁴¹ the 2,2 bipyridyl and 1,10-phenanthroline-5-amine (PMeOx/X-PANI@FTO, PMeOx/X₁-PANI@FTO, PMeOx/Y-PANI@FTO, and PMeOx/Y₁-PANI@FTO) were tested to complex Fe^{2+} ions, and the results are presented in Fig. 7. It was found that PMeOx/X-PANI@FTO and PMeOx/X₁-PANI@FTO are sensitive towards Fe^{2+} ions but in the different concentration ranges (Fig. 7a and b respectively). Note that PMeOx/X₁-PANI@FTO is more sensitive compared to PMeOx/X-PANI@FTO and exhibits a slope value of 192.67 ± 6.2 mV per decade ($n = 5$). This behavior could be explained by the method of the chelating molecules deposition. When 2,2 bipyridyl is introduced during acid-assisted polymerization of PANI it forms a composite with the PANI chains and could be more sensitive towards Fe^{2+} detection, even though in a much higher concentration range compared to the drop-casting deposition method.

The 1,10-phenanthroline-5-amine chelating agent does not have sensitivity towards Fe^{2+} ions compared to 2,2 bipyridyl (Fig. 7d) if the method of deposition is acid-assisted polymerization. The possible explanation for such behavior is unknown to us.

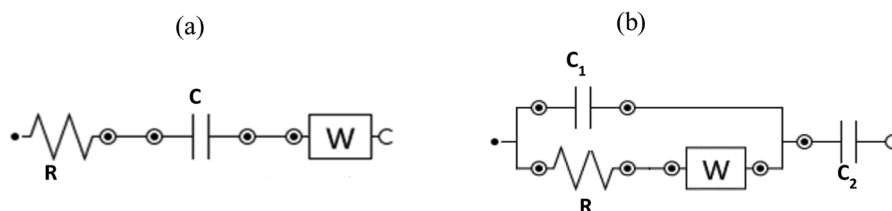
The drop-casting deposition of 1,10-phenanthroline-5-amine does not give a sensitive composite layer (Fig. 7c) compared to 2,2 bipyridyl (Fig. 7a). Only in a very narrow concentration range (25 to 50 μM) does the PMeOx/Y-PANI@FTO electrode detect Fe^{2+} ions and exhibit a slope value of 64.5 ± 2.2 ($n = 5$).

The 8-hydroxyquinoline agent is used to prepare the PMeOx/Z-PANI@FTO and PMeOx/Z₁-PANI@FTO electrodes and these electrodes were tested for Fe^{3+} ion detection, as reported earlier.⁴¹ The results of the potentiometric measurements are shown in Fig. 8. It is obvious that the PMeOx/Z₁-PANI@FTO electrode shows an immediate response to the presence of Fe^{3+} ions and has a slope value of 16.2 ± 0.6 mV per decade ($R^2 = 0.9898$, $n = 5$), and the theoretical value is 19.6 mV. Based on these results we conclude that the PMeOx/Z₁-PANI@FTO electrode is the most promising sensor for real applications.

Table 1 EIS data fitted with the equivalent circuit

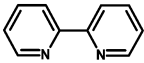
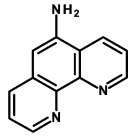
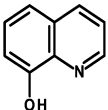
Developed sensing electrodes ^a	<i>R</i> (Ω)	<i>C</i> (mF)	<i>C</i> ₁ (nF)	<i>C</i> ₂ (mF)	<i>W</i> (mMho)	CPE (mMho s N)	Error (χ ²)
PANI@FTO	27		32	8.21	46.5		0.0040
X ₁ -PANI@FTO	26	2.81				5.93, <i>n</i> = 0.632	0.019
Y ₁ -PANI@FTO	24.1	8.35			38.9		0.011
Z ₁ -PANI-FTO	24.6	5.68			20.7		0.051
PMeOx/X ₁ -PANI@FTO	27.9		16.5	3.99	13.1		0.2911
PMeOx/Y ₁ -PANI@FTO	22.7		24.3	10.1	61		0.0742
PMeOx/Z ₁ -PANI@FTO	22.7		24.3	10.1	61		0.074
X-PANI@FTO	26.4		16	6.29	54.2		0.0756
Y-PANI@FTO	25.7		15.9	6.78	25.8		0.092
Z-PANI-FTO	27.1		16.8	12.9	32.1		0.23
PMeOx/X-PANI@FTO	24.7		23.6	8.32	43.1		0.0848
PMeOx/Y-PANI@FTO	22.7		24.3	10.1	61		0.074
PMeOx/Z-PANI@FTO	30.8		16.2	7.52	12.6		0.871

^a Models of equivalent circuits that were applied.



a) X₁-PANI@FTO, Y₁-PANI@FTO and Z₁-PANI@FTO, b) PANI@FTO, X-PANI@FTO, Y-PANI@FTO, Z-PANI@FTO, PMeOx/X-PANI@FTO, PMeOx /Y-PANI@FTO, PMeOx /Z-PANI@FTO, PMeOx/X₁-PANI@FTO, PMeOx /Y₁-PANI@FTO and PMeOx /Z₁-PANI@FTO

Table 2 The detailed names and procedures for the developed sensing electrodes

Deposited chelating molecules and PMeOx	Deposition method	Names	Quantity/volume
2,2-bipyridyl	Drop-casting <i>In situ</i> deposition	PMeOx/X-PANI@FTO PMeOx/X ₁ -PANI@FTO	(0.015 g) in 1 mL of DMSO (0.015 g) in 1 mL of HCOOH
 1,10-phenanthroline-5-amine	Drop-casting <i>In situ</i> deposition	PMeOx/Y-PANI@FTO PMeOx/Y ₁ -PANI@FTO	(0.019 g) in 1 mL of DMSO (0.019 g) in 1 mL of HCOOH
 8-hydroxyquinoline	Drop-casting <i>In situ</i> deposition	PMeOx/Z-PANI@FTO PMeOx/Z ₁ -PANI@FTO	(0.014 g) in 1 mL of ethanol (0.014 g) in 1 mL of HCOOH
			

Based on these results, our next goal was to measure the potentiometric response of PMeOx/Z₁ PANI@FTO at 37 °C, relevant to the human body, and the results of the measurements are presented in Fig. 9.

At higher temperature the slope value is 26.1 ± 1.1 mV per decade ($R^2 = 0.9791$, $n = 5$). We explain the slight decrease in sensitivity of the developed sensor PMeOx/Z₁-PANI@FTO towards Fe³⁺ ions, due to the diffusion processes that take place at higher temperatures.

Experimental

Materials

Formic acid (Sigma Aldrich, Czech Republic), ammonium peroxydisulfate (Lach-ner, Czech Republic), ethyl alcohol (99.8%, Sigma Aldrich, Czech Republic), and analytical grade aniline (Lach-ner, Czech Republic, p.a.), were used to prepare PANI films. Poly(2-methyl-2-oxazoline) was used as a non-biofouling layer and was synthesized according to ref. 33.



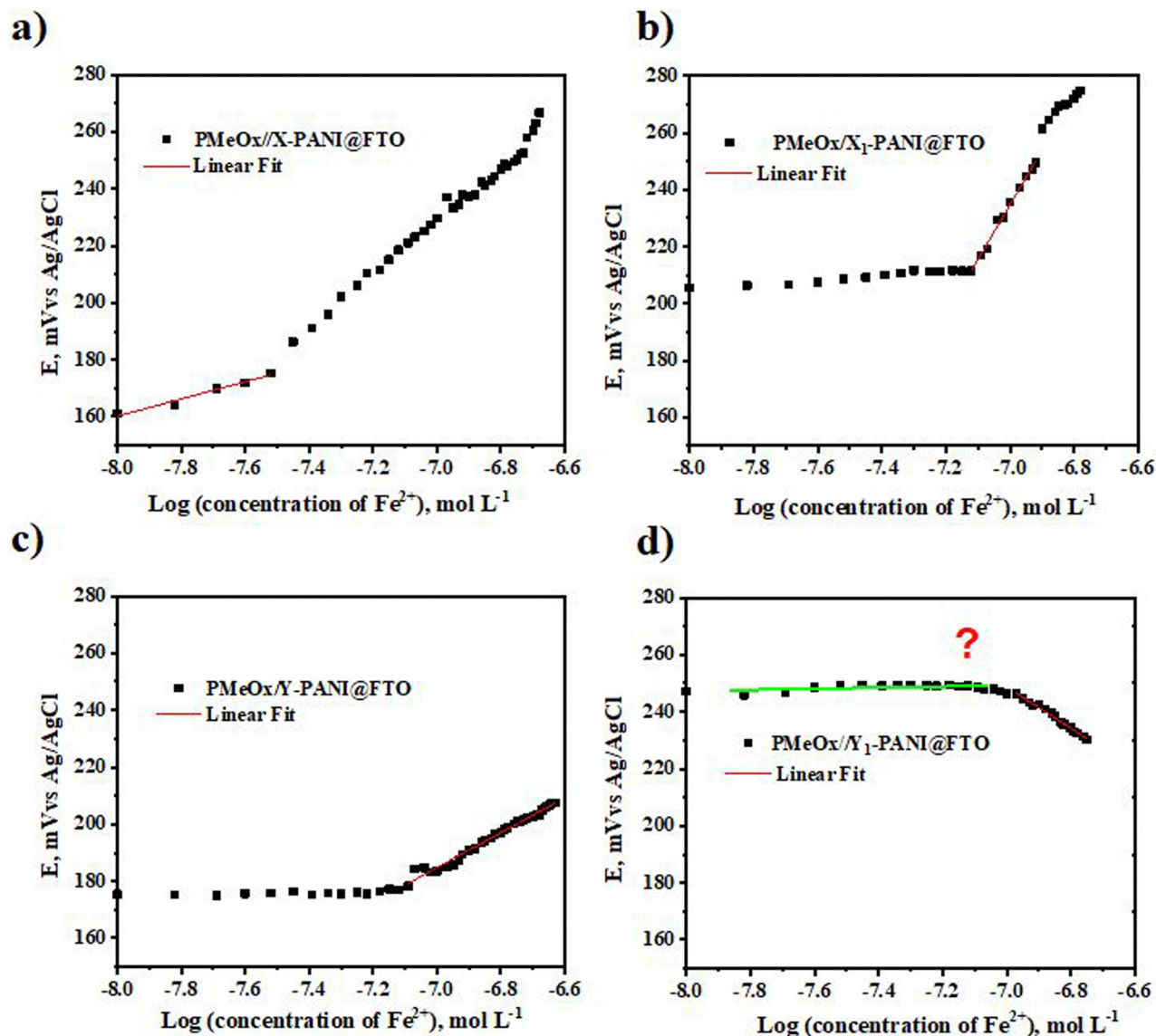


Fig. 7 Potentiometric detection of Fe^{2+} ions by PMeOx/X-PANI@FTO, PMeOx//X₁-PANI@FTO, PMeOx//Y-PANI@FTO and PMeOx/Y₁-PANI@FTO electrodes.

2,2-Bipyridyl, 1,10-phenanthroline-5-amine, and 8-hydroxyquinoline (Sigma Aldrich, Czech Republic) were used in the experiments as received without further purification. Dimethyl sulfoxide (DMSO, Lach-ner, Czech Republic), ethyl alcohol (99.8%, Sigma Aldrich, Czech Republic), and formic acid (HCOOH) were used as solvents to dissolve the chelating molecules. Iron(III)-chloride hexahydrate (Sigma Aldrich, Czech Republic) and iron(II) chloride (Sigma Aldrich, Czech Republic) were used to study the sensing ability of electrodes. FTO glass was also used as a support after washing and drying in the oven.

Synthesis of polyaniline and deposition on the FTO support (PANI@FTO)

Acid-assisted polymerization was carried out at room temperature in the presence of ammonium peroxydisulfate as follows: 0.1 mL of aniline (1.6×10^{-4} M) was dissolved in 4.7 mL of

concentrated formic acid (HCOOH) and 1 mL of ethanol ($\text{C}_2\text{H}_5\text{OH}$). Ammonium peroxydisulfate (APS: 1.02×10^{-4} M, 0.0235 g in 1 mL of water) was added, as an aqueous solution, dropwise into the mixture. The monomer to oxidant molar ratio is 1:0.1. After the polymerization was complete, the resulting solution was deposited on FTO glass by drop-casting followed by washing with 5.0 M aqueous formic acid and drying at room temperature as presented by Scheme 1a and b.

Chelating molecules

Three molecules (2,2-bipyridyl, 1,10-phenanthroline-5-amine and 8-hydroxyquinoline) were used as a chelating agent to coordinate the Fe^{2+} or Fe^{3+} ions respectively. Two methods are applied to make a composite with PANI: the 1st method corresponds to drop-casting deposition (see Scheme 1a), individual chelating molecules were dissolved in a specific solvent



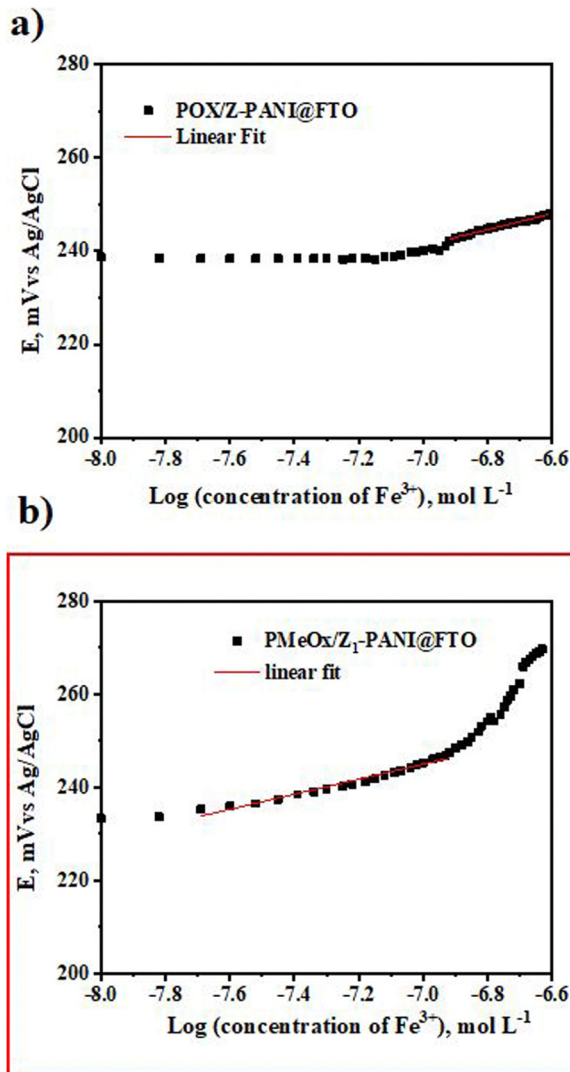


Fig. 8 Potentiometric detection of Fe^{3+} ions by PMeOx/Z-PANI@FTO and $\text{PMeOx/Z}_1\text{-PANI@FTO}$ electrodes.

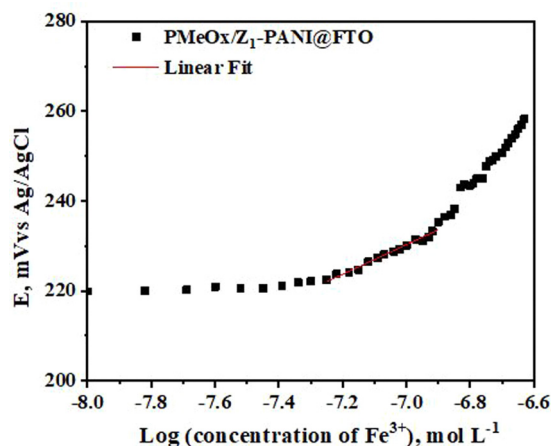


Fig. 9 Potentiometric detection of Fe^{3+} ions by $\text{PMeOx/Z}_1\text{-PANI@FTO}$ measured at 37°C .

(see Table 2) and then carefully applied to PANI@FTO film; the 2nd method is the *in situ* incorporation of chelating molecules during acid-assisted polymerization of aniline (see Scheme 1b).

Drop casting deposition of the chelating agent layer. 0.1 M of a chelating agent (see Table 1) was dissolved in 1 mL of solvent and then deposited on top of the PANI@FTO (Scheme 1). The PANI layer was firstly fixed by applying the cyclic voltammetry technique (scan rate 50 mV s^{-1} , 10 cycles) in HCl (0.1 M) before the deposition of the individual chelating molecule layer. DMSO was used as a solvent to dissolve the 2,2-bipyridyl or 1,10-phenanthroline-5-amine and ethanol was used as a solvent to dissolve the 8-hydroxyquinoline (Table 2).

The X-PANI@FTO , Y-PANI@FTO , and Z-PANI@FTO electrodes were obtained.

***In situ* incorporation of the chelating agent during acid-assisted polymerization.** The *in situ* incorporation of the chelating agent during acid-assisted polymerization of aniline was performed by dissolving 0.1 mL of aniline in 3.7 mL of concentrated formic acid and 1 mL of ethanol. Afterward, 0.1 M of a chelating agent (see Table 2) was separately dissolved in 1 mL of concentrated formic acid and added to the mixture. Then the aqueous solution of ammonium peroxydisulfate (APS, 0.0235 g in 1 mL of water) was slowly added to the mixture.

The $\text{X}_1\text{-PANI@FTO}$, $\text{Y}_1\text{-PANI@FTO}$, and $\text{Z}_1\text{-PANI@FTO}$ electrodes were obtained.

Deposition of the PMeOx layer at PANI@FTO

Non-biofouling layer poly(2-methyl-2-oxazoline) (PMeOx) solution (molecular weight of 2 kDa) was deposited on X-PANI@FTO , $\text{X}_1\text{-PANI@FTO}$, Y-PANI@FTO , $\text{Y}_1\text{-PANI@FTO}$, Z-PANI@FTO , and $\text{Z}_1\text{-PANI@FTO}$. The obtained electrodes were finally dried at room temperature followed by applying the electrochemical cyclic voltammetry method in acetonitrile in order to fix PMeOx.

Methods

The following techniques are used for the characterization of materials: Raman and X-ray photoelectron spectroscopy (XPS) spectroscopy, Electron Paramagnetic Resonance (EPR), MALDI-TOF mass spectroscopy, electrochemical techniques (cyclic voltammetry (CV), and electrochemical impedance spectroscopy (EIS)).

Raman spectra of PANI@FTO and (X-PANI@FTO , $\text{X}_1\text{-PANI@FTO}$, Y-PANI@FTO , $\text{Y}_1\text{-PANI@FTO}$, Z-PANI@FTO , and $\text{Z}_1\text{-PANI@FTO}$) were acquired on Renishaw InVia microspectrometer equipped with a Leica DM LM microscope. The spectra were measured with two excitation lines, Ag laser 514 nm and NIR diode laser 785 nm with gratings $2400\text{ lines mm}^{-1}$ and $1200\text{ lines mm}^{-1}$, respectively.

X-Ray photoelectron spectroscopy (XPS) measurements were carried out on a K-Alpha+ spectrometer (ThermoFisher Scientific, East Grinstead, UK). The samples were analysed using a micro-focused, monochromated Al $\text{K}\alpha$ X-ray source ($400\text{ }\mu\text{m}$ spot size) at an angle of incidence of 30° (measured from the surface) and an emission angle normal to the surface. The XPS spectra were fitted with Voigt profiles obtained by convolving Lorentzian and Gaussian functions.



The electron paramagnetic resonance (EPR) measurements of the PANI solution were performed using an EPR spectrometer in the X-band Bruker ELEXSYS E 500 with 100 kHz field ac modulation for phase-lock detection.

MALDI-TOF mass spectroscopy was obtained on a Bruker MALDI-TOF spectrometer using *trans*-2-[3-(4-*tert*-butylphenyl)-2-methyl-2-propenylidene] malononitrile as a matrix in the negative ionization mode. Electrochemical characterization of the electrodes was carried out in two electrode cell configurations using an AUTOLAB PGSTAT302N potentiostat with a FRA32M Module and Nova 2.1 software. A Pt sheet (1.2 cm²) was used as the counter electrode, and Ag/AgCl (3 M KCl) was used as the reference electrode. Cyclic voltammetry was measured in the potential window from −0.1 to 0.8 V vs. a Ag/AgCl reference electrode with 10 and/or 50 mV s^{−1} scan rates in an aqueous solution of H₂SO₄ (0.1 M) or HCl (0.1 M). Electrochemical impedance spectroscopy (EIS) was performed in the frequency range from 10 kHz to 0.1 Hz at open circuit potential (OCP) in aqueous solution of HCl (0.1 M).

The potentiometric measurements were performed in 0.1 M NaCl and were measured using a 6-channel high-input-impedance voltmeter with the input impedance of 1010 Ω (Lawson Laboratories, Malvern, PA, USA). The developed sensing electrodes were immersed in the solution and when the potential drift was not detected the studied ions were added (started from the low concentration); the solution was stirred for 3 min and after 4 min the signal was recorded. The measurements were done at room temperature or at $T = \sim 37^\circ\text{C}$.

Conclusions

In summary, it is shown for the first time that PANI could be synthesized by acid-assisted polymerization, which gives a stable PANI suspension. The PANI suspension can be deposited on any surface with the formation of a reproducible and stable film for various applications. It is a new synthetic way to obtain a stable PANI suspension. Up to now, the detailed mechanism of aniline polymerization is still unclear, and this is a shortcoming. However, numerous experiments are undergoing and we expect in the nearest future to come up with an explanation. The three chelating molecules (2,2-bipyridyl, 1,10-phenanthroline-5-amine, and 8-hydroxyquinoline) are introduced directly into PANI during synthesis or drop-casted on top of the already formed PANI film. The potentiometric analysis reveals that the composite, PMeOx/Zr-PANI@FTO, obtained via the *in situ* method has high sensitivity toward the detection of Fe³⁺ ions. The proposed sensors demonstrated reproducibility with a rapid response to the presence of Fe³⁺ ions, even at $T \sim 37^\circ\text{C}$. We envision that this system can contribute to the next generation of advanced bio-sensors for the potentiometric detection of iron.

Author contributions

The manuscript was written through contributions of all authors. All authors have given approval to the final version of the manuscript.

Conflicts of interest

There are no conflicts to declare.

Acknowledgements

The authors declare the following financial interest/personal relationships which may be considered as potential competing interest: Elena Tomsik reports that financial support was provided by the Czech Health Research Council, NU20-06-00424. Jan Svoboda reports that financial support was provided by the Czech Science Foundation, 20-08679S.

References

- 1 N. K. Guimard, N. Gomez and C. E. Schmidt, *Prog. Polym. Sci.*, 2007, **32**, 876–921.
- 2 K. S. Ryu, K. M. Kim, N. G. Park, Y. J. Park and S. H. Chang, *J. Power Sources*, 2002, **103**, 305–309.
- 3 H. Itoi, S. Hayashi, H. Matsufusa and Y. Ohzawa, *Chem. Commun.*, 2017, **53**, 3201–3204.
- 4 M. Kiristi and A. Uygun, Polyaniline, *Handbook of Engineering and Specialty Thermoplastics*, 2011, **4**, 183–210.
- 5 P. N. Moghadam and E. N. Zareh, *E-Polym.*, 2010, **10**(1), 054.
- 6 T. V. Freitas, E. A. Sousa, G. C. Fuzari Jr. and E. P. S. Arlindo, *Mater. Lett.*, 2018, **224**, 42–45.
- 7 Z. Tian, H. Yu, L. Wang, M. Saleem, F. Ren, P. Ren, Y. Chen, R. Sun, Y. Sun and L. Huang, *RSC Adv.*, 2014, **4**, 28195–28208.
- 8 C. Yin, L. Gao, F. Zhou and G. Duan, *Polymers*, 2017, **9**, 544.
- 9 Y. Dong, Y. Zhou, Y. Ding, X. Chu and C. Wang, *Anal. Methods*, 2014, **6**, 9367–9374.
- 10 J.-C. Lacroix, J.-L. Camalet, S. Aeiach, K. Chane-Ching, J. Petitjean, E. Chauveau and P.-C. Lacaze, *J. Electroanal. Chem.*, 2000, **481**, 76–81.
- 11 G. Ćirić-Marjanović, B. Marjanović, M. Popović, V. Panić and V. Mišković-Stanković, *Russ. J. Electrochem.*, 2006, **42**, 1358–1364.
- 12 M. M. Gvozdenović and B. N. Grgur, *Prog. Org. Coat.*, 2009, **65**, 401–404.
- 13 G. Inzelt, *A New Era in Electrochemistry, Conducting Polymers*, 2008, 265–269.
- 14 J. Lippe and R. Holze, The anion-specific effect in the overoxidation of polyaniline and polyindoline, *J. Electroanal. Chem.*, 1992, **339**, 411–422, DOI: [10.1016/0022-0728\(92\)80465-G](https://doi.org/10.1016/0022-0728(92)80465-G).
- 15 P. Nunziante and G. Pistoia, *Electrochim. Acta*, 1989, **34**, 223–228.
- 16 M. M. Gvozdenović, B. Z. Jugović, J. S. Stevanović, T. L. Trišović and B. N. Grgur, *Electrochemical polymerization of aniline, Electropolymerization*, Intech, 2011.
- 17 S. Bhadra, D. Khastgir, N. K. Singha and J. H. Lee, *Prog. Polym. Sci.*, 2009, **34**, 783–810.
- 18 C. M. Zhu, Y. He, Y. J. Liu, N. Kazantseva, P. Saha and Q. Cheng, *J. Energy Chem.*, 2019, **35**, 124–131.



- 19 H. Zou, L. Wang, X. Wang, P. Lv and Y. Liao, *Polymers*, 2016, **8**, 407–417.
- 20 W. Chen, R. B. Rakhi and H. N. Alshareef, *J. Phys. Chem. C*, 2013, **117**, 15009–15019.
- 21 B. Xu, X. B. Wang, Y. Y. Huang, J. Liu, D. Wang, S. J. Feng, X. H. Huang and H. T. Wang, *Chem. Eng. J.*, 2020, **399**, 125749.
- 22 Y. Ma, H. Zhang, C. Hou, M. Qiao, Y. Chen, H. Zhang and Q. Zhang, *J. Mater. Sci.*, 2017, **52**, 2995–3002.
- 23 B. W. Qiu, J. Y. Wang, Z. J. Li, X. Wang and X. Y. Li, *Polymers*, 2020, **12**, 310–323.
- 24 V. Babel and B. L. Hiran, *Polym. Compos.*, 2021, **42**, 3142–3157.
- 25 T. Das and B. Verma, *J. Mater. Sci.: Mater. Electron.*, 2022, **33**, 12734–12749.
- 26 Y. Shen, Z. Qin, T. Li, F. Zeng, Y. Chen and N. Liu, *Electrochim. Acta*, 2020, **356**, 136841.
- 27 S. Cho, K. H. Shin and J. Jang, *ACS Appl. Mater. Interfaces*, 2013, **5**, 9186–9193.
- 28 W. Li and H. L. Wang, *J. Am. Chem. Soc.*, 2004, **126**, 2278–2279.
- 29 X. Zhang, W. Goux and S. Manoha, *J. Am. Chem. Soc.*, 2004, **126**, 4502–4503.
- 30 K. Komaba and H. Goto, *Polym.-Plast. Technol. Mater.*, 2021, **60**, 906–9016.
- 31 E. Tomšík, Z. Morávková, J. Stejskal, M. Trchová and J. Zemek, *Synth. Met.*, 2012, **162**, 2401–2405.
- 32 A. E. ElMetwally, M. S. Sayed, E. Zeynaloo, E. M. Zahran, J. J. Shim, M. R. Knecht and L. G. Bachas, *J. Phys. Chem. C*, 2022, **126**, 2503–2516.
- 33 H. Zhang, H. X. Li and H. M. Cheng, *J. Phys. Chem. B*, 2006, **110**, 9095–9099.
- 34 J. X. Feng, S. Y. Tong, Y. X. Tong and G. R. Li, *J. Am. Chem. Soc.*, 2018, **140**, 5118–5126.
- 35 B. H. Lee, H. J. Kim and H. S. Yang, *Curr. Appl. Phys.*, 2012, **12**, 75–80.
- 36 J. X. Deng, T. M. Wang, J. S. Guo and P. Liu, *Prog. Nat. Sci.: Mater. Int.*, 2017, **27**, 257–260.
- 37 F. Kelly, J. Johnston, T. Borrmann and M. Richardson, *Eur. J. Inorg. Chem.*, 2007, 5571–5577.
- 38 R. Mažeikiene, G. Niaura and A. Malinauskas, *J. Solid State Electrochem.*, 2019, **23**, 1631–1640.
- 39 T. Trung, T. H. Trung and C. S. Ha, *Electrochim. Acta*, 2005, **51**, 984–990.
- 40 I. Ivanko, T. Lindfors, R. Emanuelsson and M. Sjödin, *Sens. Actuators, B*, 2021, **329**, 129231.
- 41 R. Ismail, I. Šeděnková, Z. Černochohá¹, O. Pop-Georgievski, I. Romanenko¹, M. Hrubý and E. Tomšík, *Biosensors*, 2022, **12**, 446.

